Pitfalls in shaker vibration tests on lightweight structures

C. Schedlinski
ICS Engineering GmbH,
Am Lachengraben 5, D-63303 Dreieich, Germany
E-Mail: **info@ics-engineering.com**

Abstract
This publication highlights typical pitfalls when using shaker excitation to test lightweight structures and illustrates the basic phenomena using a simple practical example. The main issues are mass loading and stinger interferences, which can lead to considerable distortions of the test data sought. The overall aim is to make the test engineer aware of the topic and to provide guidance for test planning of a shaker test on lightweight structures.

1 Introduction

For vibration tests on lightweight structures the proper selection of the excitation method can be a challenging task, especially when an automatable excitation, e.g. by a shaker system, is required. This may for instance be the case if a laser scanner measurement with high spatial resolution is to be conducted where manual excitation of the system is no longer appropriate.

Now, the shaker system, its connection to the test item (stinger), and the required load cell for force measurement can significantly alter the system dynamics. The main reasons for this are the mass loading from the load cell and parasitic excitations in lateral and rotational directions that are not measured by the load cell. Especially the latter can lead to a (partial) coupling of stinger and shaker to the original system that can even introduce additional modes that are not present in the original system.

Thus, usually a well decoupled connection is sought (stiff in axial direction and flexible in lateral and rotational directions) that is not always easy to achieve. Therefore, an appropriate stinger selection/design before the test is a key issue for obtaining reliable test data. Furthermore, if the test data are to be used for comparison with FE data, an introduction of load cell, stinger, and/or shaker into the FE model may have to be considered.

By means of a real-life example the basic effects are highlighted and discussed that may be introduced by the excitation system. A dedicated hammer test will serve as baseline, next to a validated FE model of the selected test item. Especially, systematic errors that may originate from the shaker attachment will be shown and strategies for a reduction of these are presented.

The overall goal is to make the test engineer aware of the topic and to provide guidance for test design of a shaker test on lightweight structures.

2 Use Case: Cover Plate

Figure 1 shows the cover plate that will be investigated in the following to highlight the basic phenomena to be respected when testing lightweight structures with shaker excitation. The cover plate has an overall mass of about 860g and measures approximately 305x165x33mm.

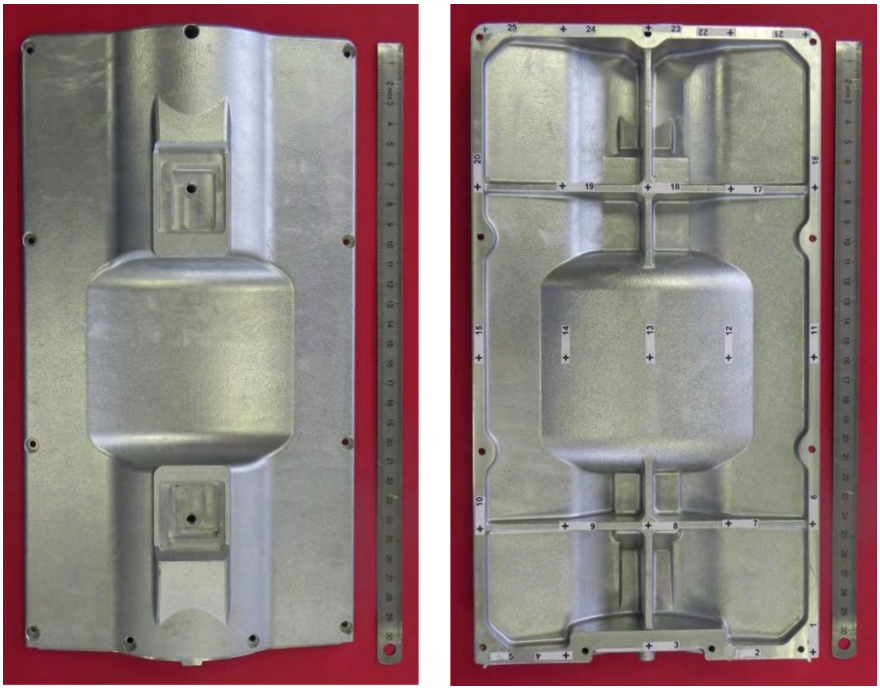

Figure 1: Cover plate (≈860g, ≈305x165x33mm)

For this cover plate a solid FE model was created (Figure 2) that yields 13 elastic modes up to 4kHz in free/free configuration and which was subsequently used for test planning and test/analysis correlation. In particular, a reduced test model with 25 measurement nodes was derived (Figure 3), that sufficiently represents the modes up to 4kHz spatially when perpendicular measurements are taken. This is demonstrated by the Auto-MAC matrix in Figure 4, calculated for the 25 perpendicular measurement degrees of freedom (MDOF) alone.

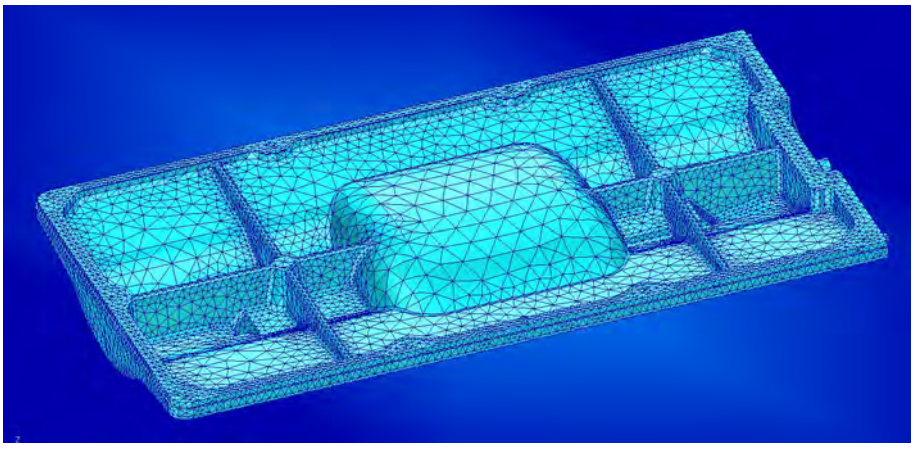

Figure 2: Survey of FE model

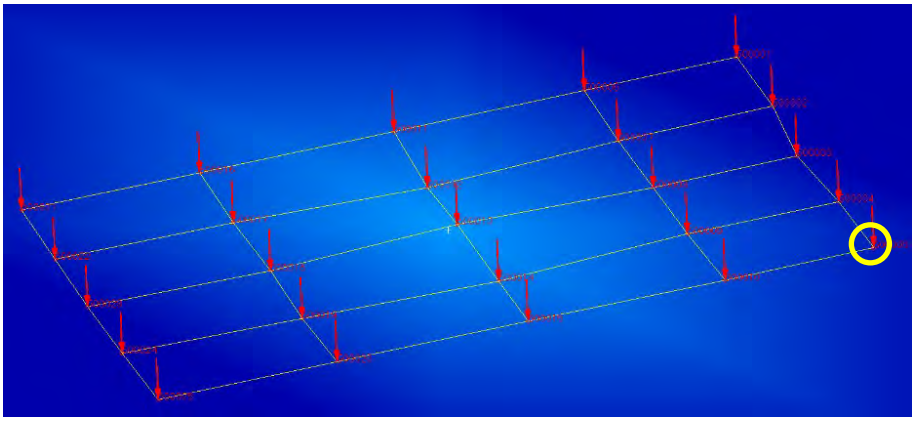

Figure 3: Test model with selected measurement degrees of freedom

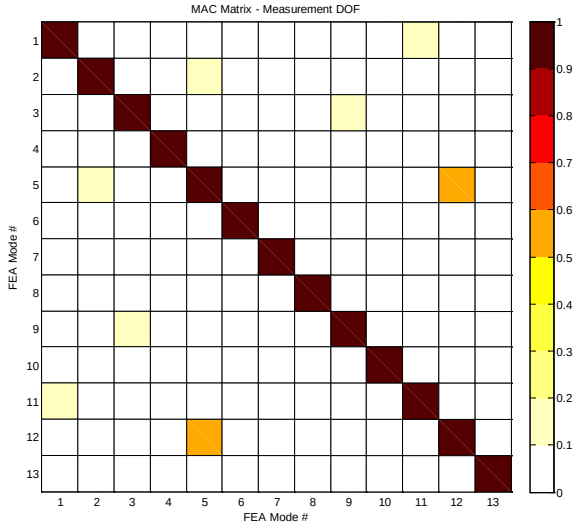

Figure 4: FEA Auto-MAC calculated for the 25 perpendicular measurement degrees of freedom alone

Sufficient excitation of all modes up to 4 kHz can be introduced e.g. at measurement node 500005 (yellow circle in Figure 3 above) which can be seen from the MIF (mode indicator function) plot in Figure 5.

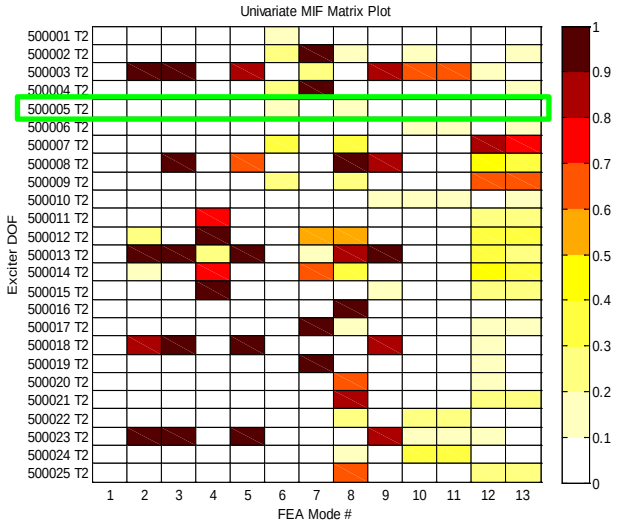

Figure 5: Univariate MIF values at natural frequencies for all 25 measurement degrees of freedom

3 Test Data

Now, for the cover plate several modal tests have been conducted to investigate step-by-step the individual influences of load cell, stinger, and stinger connection to the base structure. The tests in detail were:

1. Roving hammer test with fixed mini uniaxial acceleration sensors (baseline test)
2. Roving laser vibrometer test with fixed hammer excitation (comparison acceleration/laser)
3. Repetition of 2. with added load cell (hammer excitation via impact cap on load cell, measurement of hammer force *and* load cell force)
4. Roving laser vibrometer test with fixed shaker excitation and vinyl stinger (ultra-flexible stinger)
5. Roving laser vibrometer test with fixed shaker excitation and steel stinger (ultra-stiff stinger)

The tests and their results are described in the following sections.

3.1 Test 1 (Roving Hammer)

Test 1 has been conducted as a classical roving hammer test with two mini uniaxial acceleration sensors with a mass of 0.2g each (without cable) permanently attached to the cover plate (elastically suspended by bungee cords). These sensors serve as references, one at the selected excitation point 500005, and one as a backup at point 500002. A survey of the test setup is given in Figure 6.

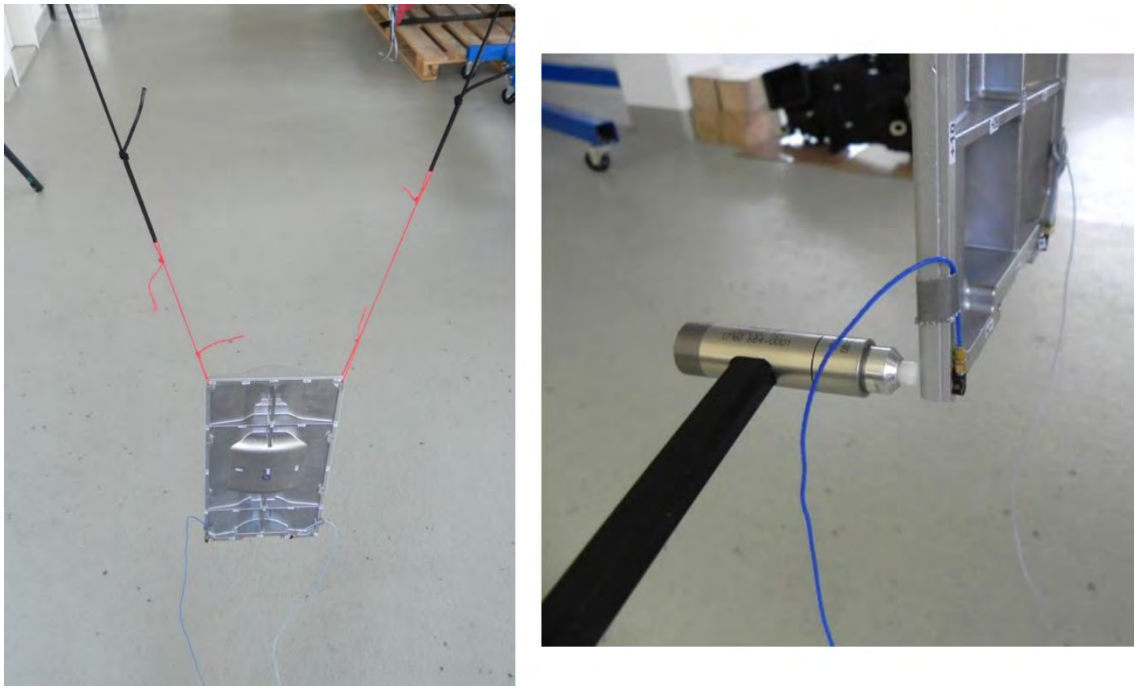

Figure 6: Base line hammer test 1

Frequency response functions (FRFs) were obtained up to 6.4kHz with a frequency resolution of 0.25Hz. Figure 7 shows a survey of all FRFs for reference 500005 up to 2kHz. Here, five clear and pronounced peaks can be found for which modal data were identified subsequently (for simplicity and without limitation for the investigations in this publication the frequency range will be restricted to 2kHz in the following), see also Table 1.

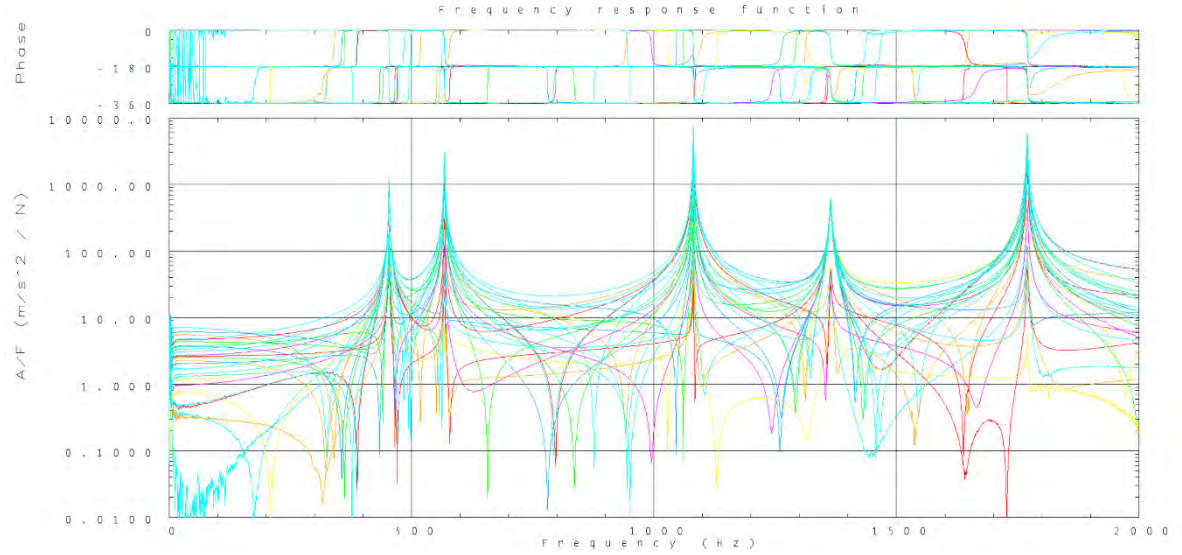

Figure 7: Test 1 – all FRFs for reference 500005

Table 1: Test 1 – modal data up to 2kHz

No	Freq. in Hz	Mod. Mass in kg	Mod. Damp. in %
1	453.38	0.33	0.09
2	567.88	0.12	0.12
3	1081.14	0.16	0.05
4	1364.32	0.48	0.13
5	1770.01	0.16	0.07

To counter check the data a test/analysis correlation was made with the FE model introduced above. The results are shown in Table 2 and Figure 8 below. It can be seen that the model and the real cover plate match very well. This could be expected from the highly detailed FE model in case of high-quality modal data from the test. Therefore, it can be concluded that the test data are of high quality and that the baseline test is well suited to track and evaluate the changes to the cover plate structure to be introduced in the following.

Table 2: Test 1 – test/analysis correlation

No	EMA	FEA	EMA in Hz	FEA in Hz	Dev. in %	MAC in %
1	1	7	453.38	458.44	1.12	99.79
2	2	8	567.88	573.60	1.01	99.00
3	3	9	1081.14	1074.23	-0.64	98.69
4	4	10	1364.32	1374.01	0.71	99.50
5	5	11	1770.01	1787.64	1.00	98.30

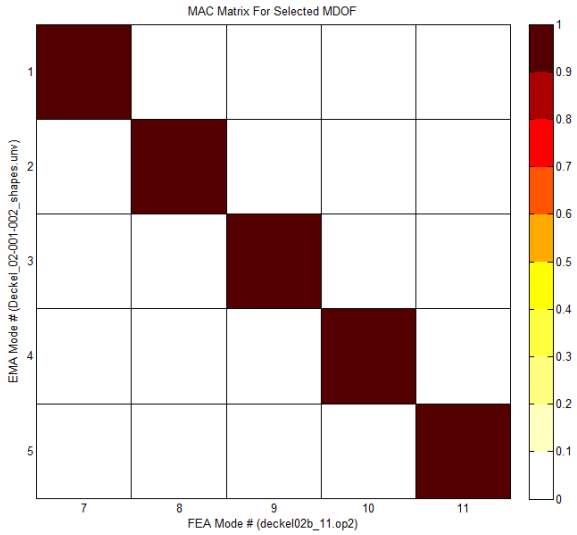

Figure 8: Test 1 – test/analysis MAC matrix

3.2 Test 2 (Roving Laser/Fixed Hammer)

For the following tests roving excitation must be exchanged by excitation at a fixed excitation point since this will be the case for the shaker tests later on as well. Now, roving acceleration sensors, even if lightweight, are usually prohibitive for lightweight test items because of the permanent change of mass loading throughout the test. These mass changes can lead to frequency shifts in the resonance peak regions that can effectively degrade the quality of the estimated modal data. Thus, a roving laser vibrometer test was conducted next and compared to the baseline test 1. Hammer excitation was applied at point 500005 in the same manner as for the preceding baseline test (see also Figure 6, right).

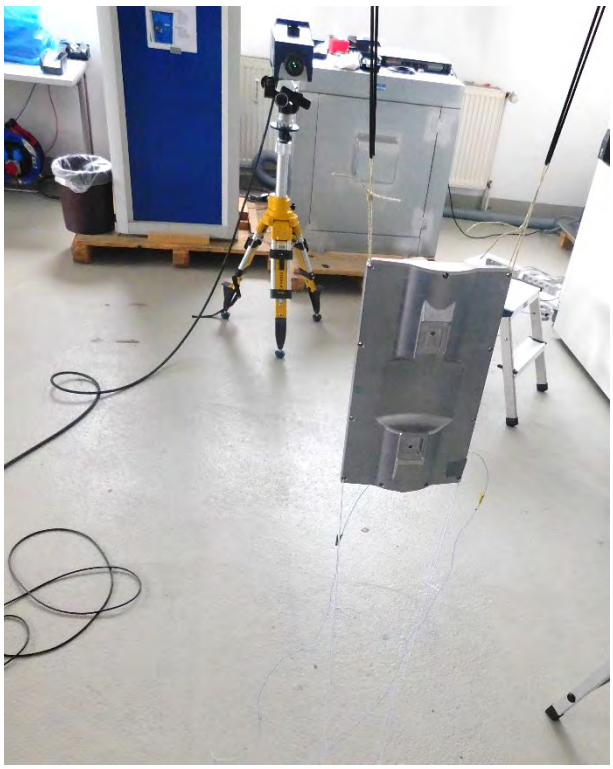

Figure 9: Roving laser test 2

In Table 3 the modal data for test 2 up to 2kHz are presented, while Table 4 shows the correlation results with test 1. It can be seen that the results from both tests are practically identical. Therefore, using roving laser vibrometer measurements in the following is equivalent to the baseline test.

Table 3: Test 2 – modal data up to 2kHz

No	Freq. in Hz	Mod. Mass in kg	Mod. Damp. in %
1	453.27	0.15	0.09
2	567.96	0.12	0.09
3	1080.92	0.05	0.08
4	1364.19	0.48	0.14
5	1769.81	0.17	0.07

Table 4: Test 2 – correlation with test 1

No	EMA1	EMA2	EMA1 in Hz	EMA2 in Hz	Dev. in %	MAC in %
1	1	1	453.38	453.27	-0.02	98.69
2	2	2	567.88	567.96	0.01	99.76
3	3	3	1081.14	1080.92	-0.02	99.17
4	4	4	1364.32	1364.19	-0.01	99.59
5	5	5	1770.01	1769.81	-0.01	99.41

3.3 Test 3 (With Load Cell)

After verification of the baseline test, a load cell was added to the cover plate in a next step. In detail, a PCB 208C02 load cell with a nominal mass of 22.7g was attached to the cover plate using instant glue (Figure 10). In addition, an impact cap with about 2.5g was bolted to the upper end of the force cell, totaling to an overall added mass of 25g which is about 3% of the mass of the cover plate.

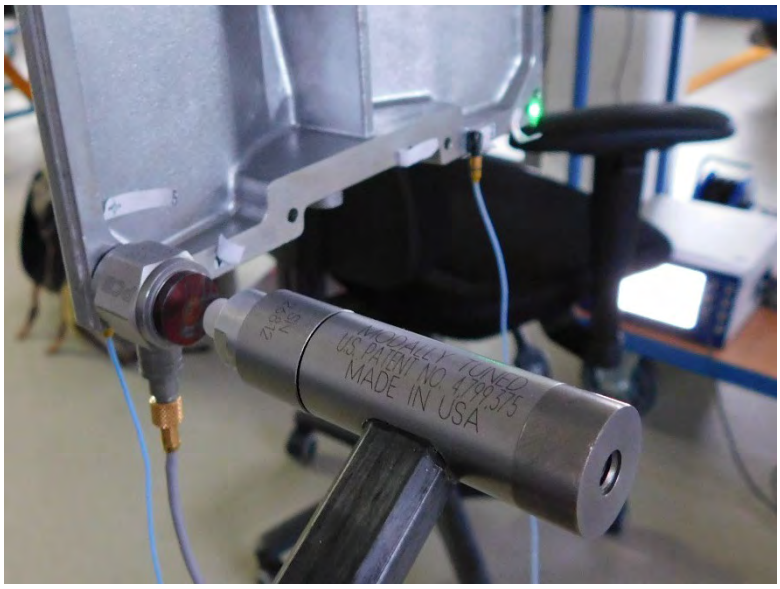

Figure 10: Load cell attached to cover plate at point 500005 with hammer excitation on impact cap

The cover plate was excited using hammer excitation as before while the hammer hits were placed directly on the impact cap (Figure 10). During the test the force signals were recorded for the impact hammer as well as for the force cell. This opened up the possibility to estimate FRFs with respect to either the impact hammer itself (i.e. the total mass of the load cell + impact cap will become part of the test item) or with respect to the load cell alternatively (i.e. only the inertia part of the load cell beyond the force measurement plane will become part of the test item, as it is the case for shaker tests).

Figure 11 exemplarily shows the reference FRFs for the baseline test, for test 3 with respect to the hammer impact, and for test 3 with respect to the load cell. The mass loading effect is obvious: even for the latter variant (blue curve), where only a fraction of the load cell mass became part of the test item, exhibits significant frequency shifts. Also, a decrease of the amplitudes can be observed which can be due to the increased inertia at the reference point or also due to friction increased damping from micro-slip in the interface region of the load cell base and the cover plate.

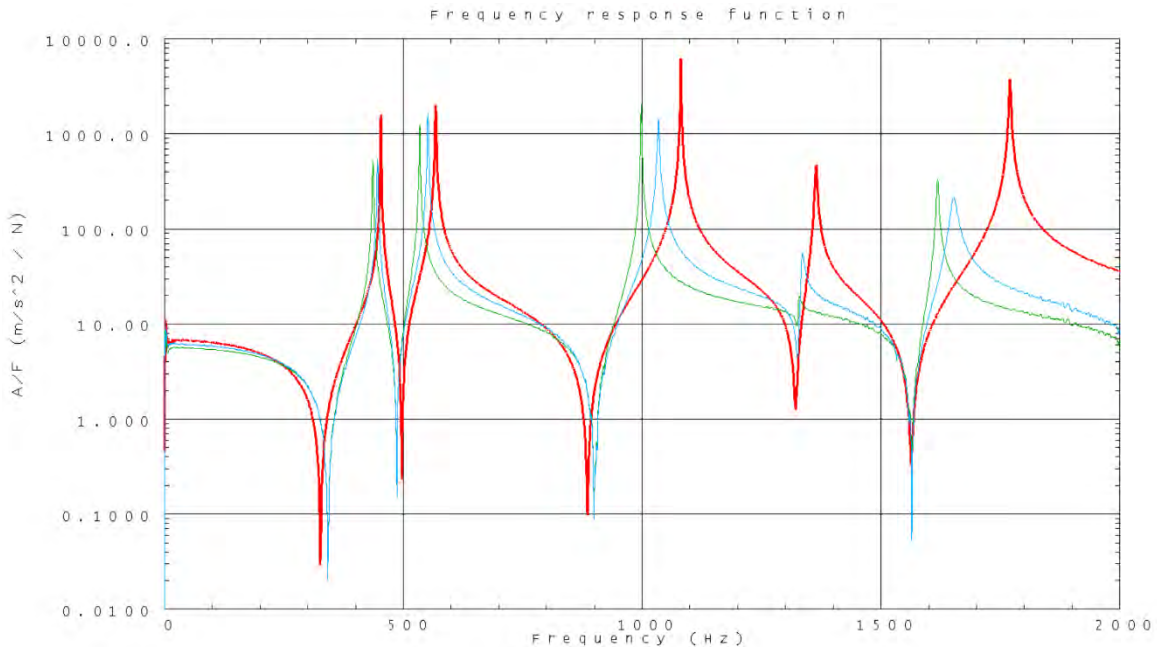

Figure 11: Test 3 - mass loading from load cell, red: baseline, green: FRF_{hammer}, blue: $FRF_{load\ cell}$

From Tables 5 and 6 the frequency shifts can directly be noticed when comparing with Table 1. Also, a certain increase in damping can be recognized. Now, as a consequence, a correlation with the FE model will obviously become worse as well, when the effects are not incorporated in the FE analysis. For the mass loading this is rather easy: adding a concentrated mass at the measurement location will capture the mass loading effect. For damping, however, this is more difficult, since no reliable estimate of the degree of damping can be made. As long as mode shapes are of concern this may not be critical. If forced responses are to be calculated, however, appropriate damping must be defined in the FE model as well.

Table 5: Test 3 – modal data up to 2kHz, FRFs related to impact hammer

No	Freq. in Hz	Mod. Mass in kg	Mod. Damp. in %
1	436.64	0.17	0.19
2	534.48	0.13	0.12
3	998.52	0.11	0.07
4	1327.81	0.00	0.18
5	1618.59	0.10	0.13

Table 6: Test 3 – modal data up to 2kHz, FRFs related to load cell

No	Freq. in Hz	Mod. Mass in kg	Mod. Damp. in %
1	446.23	0.23	0.16
2	551.64	0.14	0.13
3	1034.22	0.12	0.15
4	1335.17	0.08	0.24
5	1652.03	0.13	0.41

The effects on the test/analysis correlation are exemplarily demonstrated by comparing the modal data from the FRFs related to the impact hammer to the FE results already discussed above. In Table 7 and Figure 12 the results are shown: in this case frequency errors of about 5-10% occur and the MAC values drop below 90% or 80% respectively for two of the modes.

Table 7: Test 3 – test/analysis correlation, FRFs related to impact hammer

No	EMA	FEA	EMA in Hz	FEA in Hz	Dev. in %	MAC in %
1	1	7	436.64	458.44	4.99	94.52
2	2	8	534.48	573.60	7.32	94.02
3	3	9	998.52	1074.23	7.58	91.34
4	4	10	1327.81	1374.01	3.48	89.40
5	5	11	1618.59	1787.64	10.44	79.51

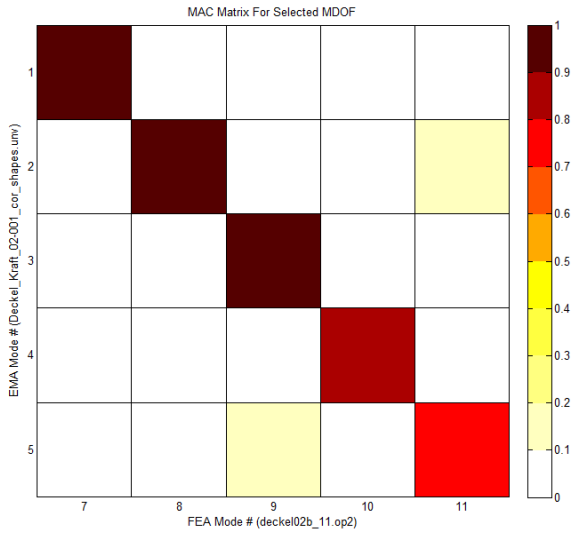

Figure 12: Test 3 – test/analysis MAC matrix, FRFs related to impact hammer

Now, in Table 8 the test/analysis correlation results are shown, when the nominal mass of the load cell + impact cap is introduced into the FE model simply as a lumped mass at the (assumed) center of gravity of the load cell: the frequency deviations are significantly reduced and the MAC values are increased. All in one the deviations are now in the order of the deviations of the baseline test compared to the initial model. Thus, correction of the systematic error of the FE model introduced by the load cell is mandatory to obtain valid test/analysis correlation results.

Table 8: Test 3 – test/analysis correlation, FRFs related to impact hammer, load cell considered in FE model

No	EMA	FEA	EMA in Hz	FEA in Hz	Dev. in %	MAC in %
1	1	7	436.64	441.22	1.05	99.23
2	2	8	534.48	539.56	0.95	99.59
3	3	9	998.52	991.43	-0.71	99.24
4	4	10	1327.81	1351.23	1.76	97.27
5	5	11	1618.59	1662.08	2.69	97.36

3.4 Tests 4 & 5 (Shaker)

Tests 4 and 5 mark, to some extent, the limiting cases of stinger options in order to highlight the basic features of stinger attachment. Figure 13, left, shows the vinyl stinger used in test 4 (very flexible), Figure 13, right, the steel stinger used in test 5 (very stiff). For the stinger tests, additional MDOF were placed on the stingers themselves in order to capture their contribution to the overall mode shapes.

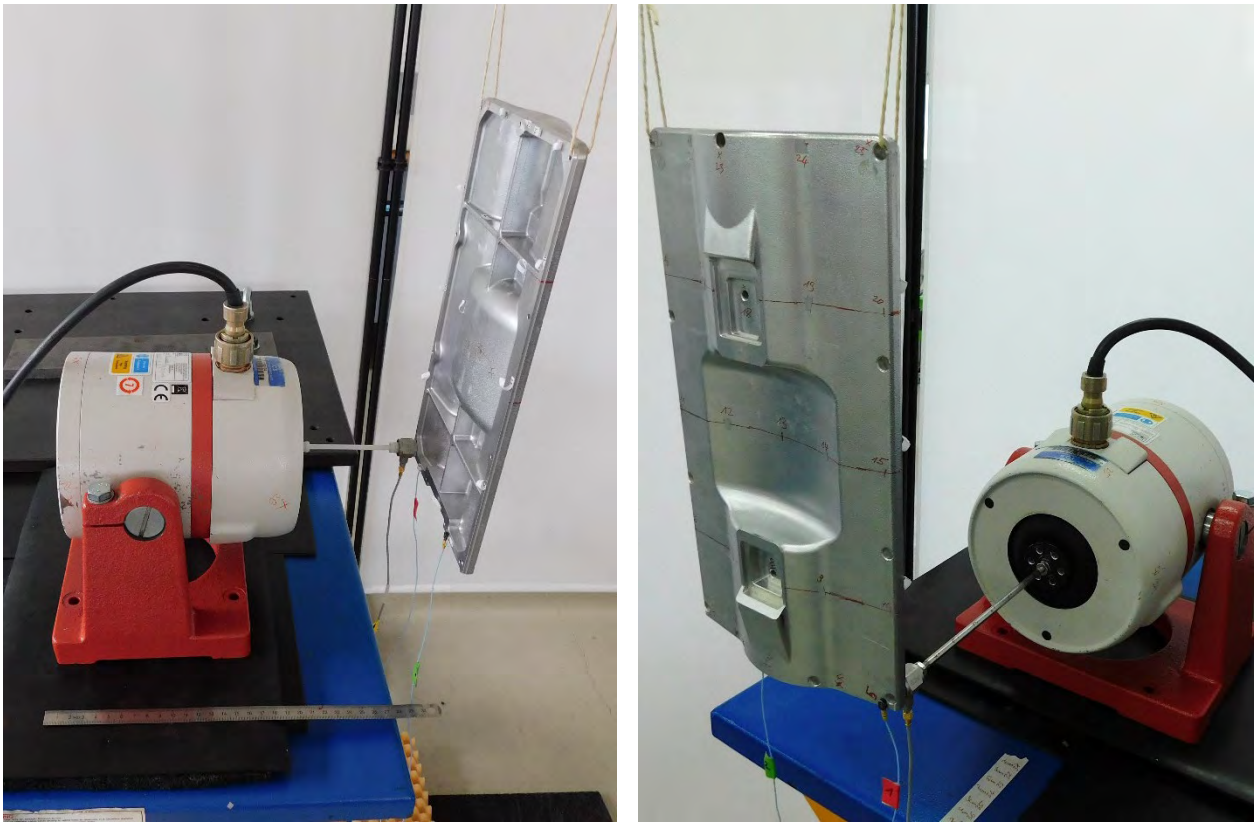

Figure 13: Survey of test 4 (left): vinyl stinger, and test 5 (right): steel stinger

Figure 14a shows the reference FRF for test 3 with respect to the load cell (→ baseline for shaker tests) in comparison to the corresponding FRFs from test 4 (vinyl), and test 5 (steel). First, it can be noted that the rigid body modes increase in frequency with increasing stiffness of the stingers (Figure 14b: FRF detail and Figure 15: typical rigid body shapes for test 5). This is due to the transverse and rotational stiffnesses of the stingers that are not eliminated by the solely axial force measurement of the load cell. That in itself is not yet a problem as long as the separation of the highest rigid body frequency and the lowest elastic frequency is large enough (a factor of 5-10 is usually considered sufficient).

Second, frequency and damping shifts can be observed, while the effects are much more pronounced for the steel stinger. Also, for the steel stinger a new resonance can be observed at around 820Hz. To further investigate this, Figure 16 shows two FRFs on the vinyl stinger and the steel stinger respectively, located next to the load cell. Here, an additional resonance can be noticed also for the vinyl stinger, although with much higher damping. Obviously, this mode is still sufficiently decoupled from the cover plate which is why it does not show in the cover plate FRFs themselves.

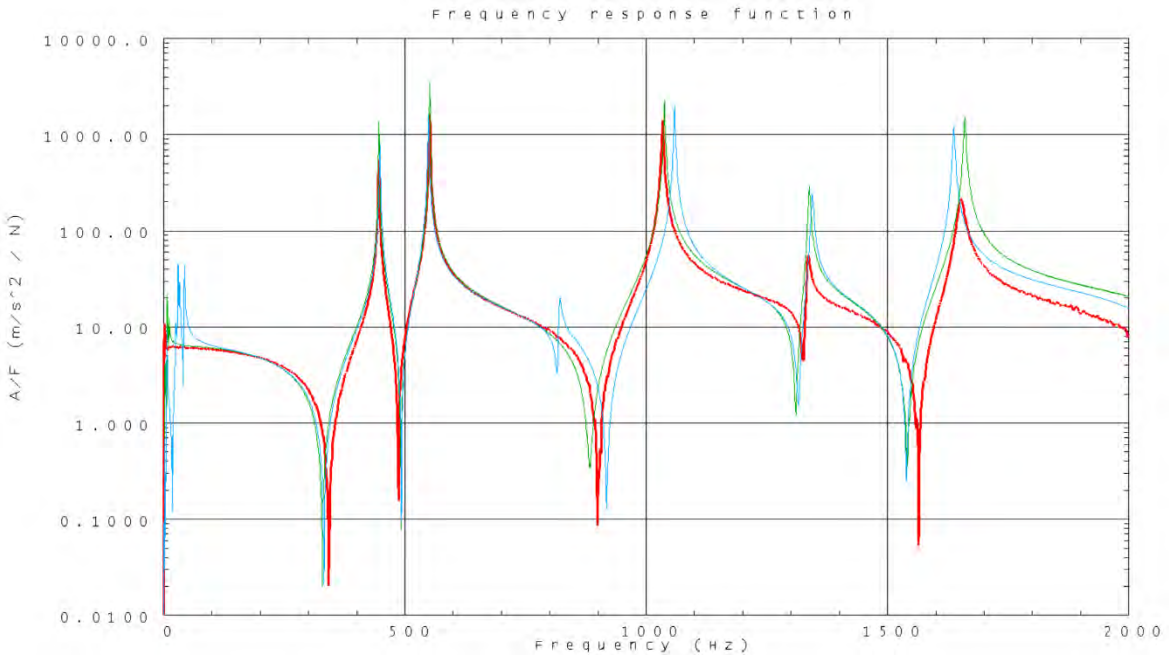

Figure 14a: Reference FRFs, red: test 3 $FRF_{load\ cell}$, green: test 4 (vinyl), blue: test 5 (steel)

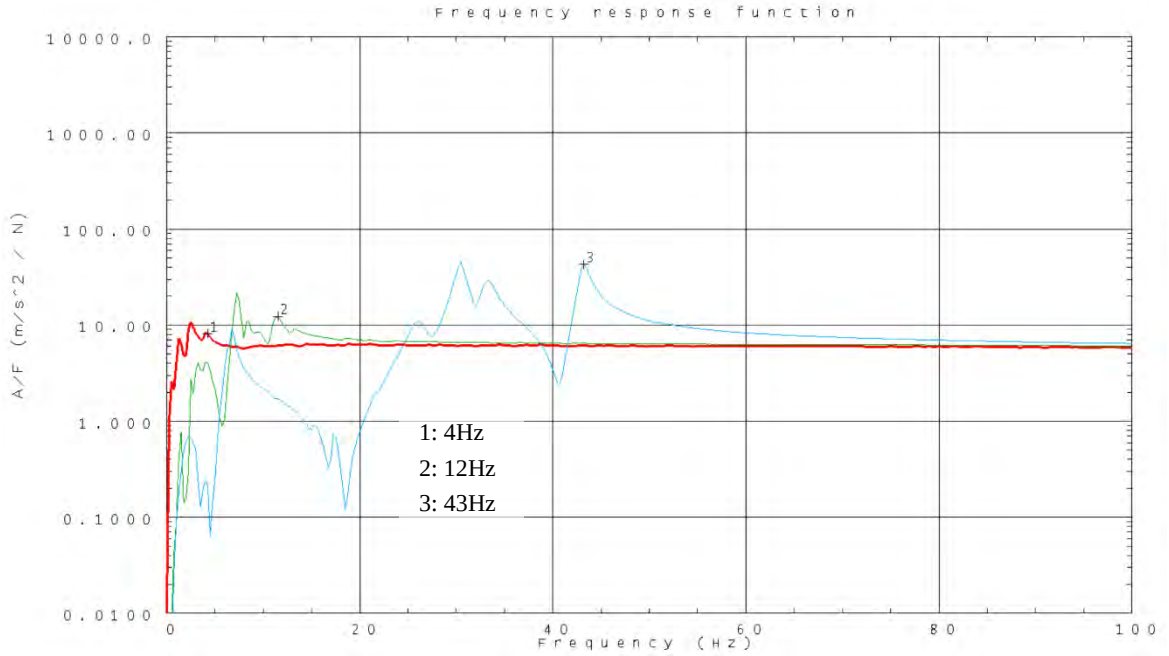

Figure 14b: Detail - Reference FRFs, red: test 3 $FRF_{load\ cell}$, green: test 4 (vinyl), blue: test 5 (steel)

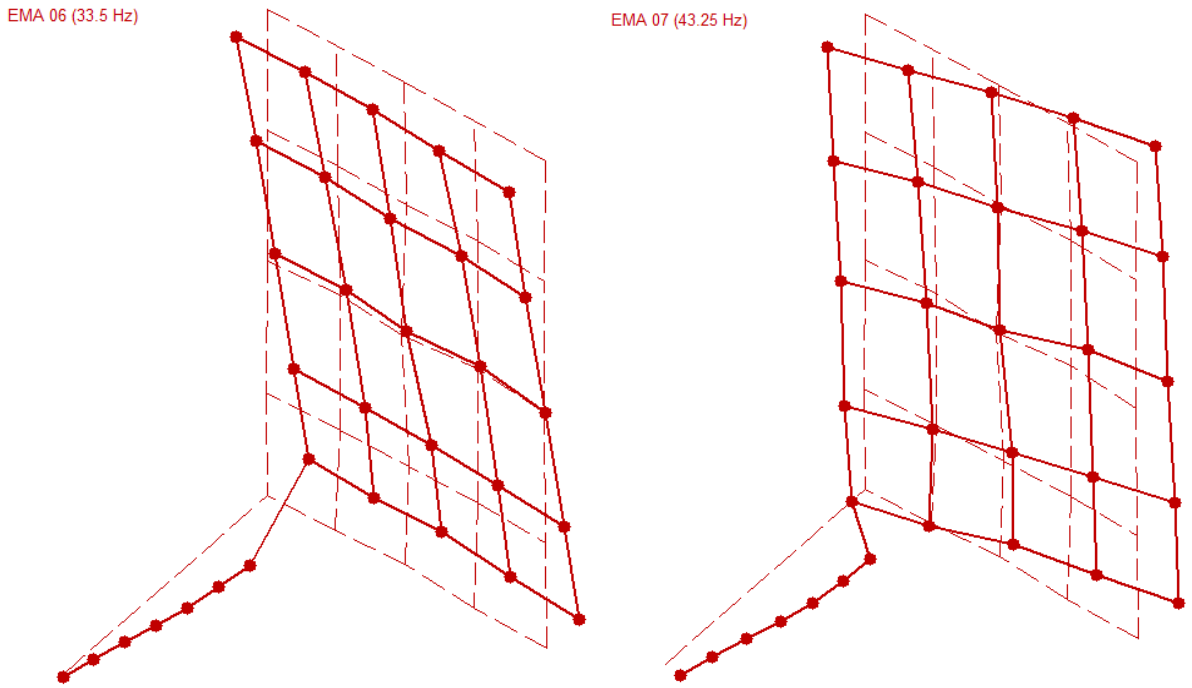

Figure 15: Test 5 (steel): exemplary rigid body modes due to stinger attachment

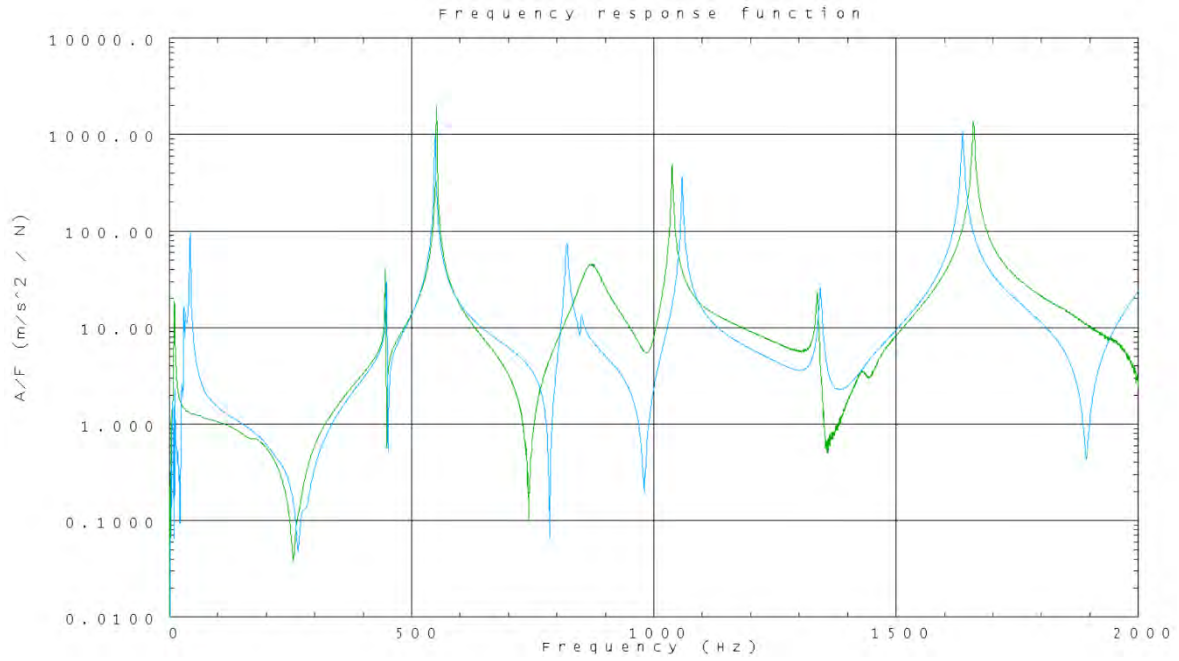

Figure 16: FRFs on stinger, green: test 4 (vinyl), blue: test 5 (steel)

In Tables 9 and 10 the modal data extracted from the FRFs of test 4 and 5 are shown. The additionally found modes of the stingers are highlighted. Tables 11 and 12 show the corresponding correlations to test 3 with respect to the load cell. It can be seen that the frequency deviations of test 3 vs. test 4 are very moderate and practically no effect on the first three MAC values of the mode shapes can be observed. Thus, the impact of the flexible vinyl stinger is more or less negligible (in the observed frequency range), at least for the natural frequencies and mode shapes. For test 3 vs. test 5 the impact on the mode shapes is only slightly higher. For the frequency deviations, however, the effect of the stinger becomes more obvious: the deviations become

larger and are not really consistent with respect to shifting frequencies up or down. Thus, the impact of the steel stinger is more prominent.

Table 9: Test 4 (vinyl) – modal data up to 2kHz, vinyl stinger (additional stinger modes highlighted)

No	Freq. in Hz	Mod. Mass in kg	Mod. Damp. in %
1	446.31	0.35	0.08
2	551.82	0.14	0.05
3	864.07	0.01	2.03
4	1037.95	0.08	0.11
5	1338.04	0.22	0.15
6	1660.24	0.15	0.11

Table 10: Test 5 (steel) – modal data up to 2kHz, steel stinger (additional stinger modes highlighted)

No	Freq. in Hz	Mod. Mass in kg	Mod. Damp. in %
1	448.55	0.35	0.14
2	548.88	0.19	0.08
3	820.60	0.01	0.30
4	850.60	3.45	0.26
5	1059.08	0.13	0.10
6	1344.11	0.34	0.17
7	1637.60	0.18	0.11

Table 11: Correlation of test 3 (FRFs related to load cell) and test 4 (vinyl)

No	EMA3	EMA4	EMA3 in Hz	EMA4 in Hz	Dev. in %	MAC in %
1	1	1	446.23	446.31	0.02	99.14
2	2	2	551.64	551.82	0.03	99.68
3	3	4	1034.22	1037.95	0.36	99.31
4	4	5	1335.17	1338.04	0.21	97.05
5	5	6	1652.03	1660.24	0.50	96.67

Table 12: Correlation of test 3 (FRFs related to load cell) and test 5 (steel)

No	EMA3	EMA5	EMA3 in Hz	EMA5 in Hz	Dev. in %	MAC in %
1	1	1	446.23	448.55	0.52	99.12
2	2	2	551.64	548.88	-0.50	99.76
3	3	5	1034.22	1059.08	2.40	98.87
4	4	6	1335.17	1344.11	0.67	96.64
5	5	7	1652.03	1637.60	-0.87	97.06

Finally, Figure 17 shows three typical modes for test 5 highlighting the contribution of the stinger to the overall mode shapes. It can clearly be seen that the stinger becomes part of the test item. Considering again the correlations discussed above, it can be concluded, that – if the stinger mode frequency (here 820Hz, Figure 17, mid) should move closer to one of the surrounding cover plate modes – the impact on the cover plate mode shapes and the MAC values will become much more pronounced.

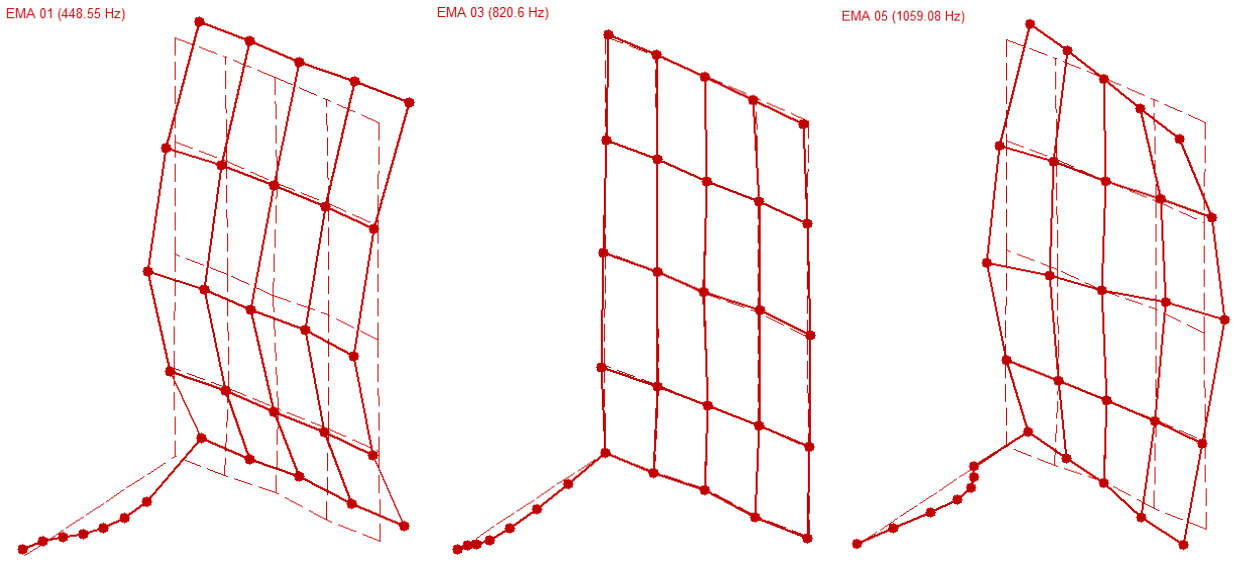

Figure 17: Test 5 (steel): exemplary elastic modes with stinger contribution

4 Summary and Conclusion

Using the example of a cover plate the basic effects of stinger attachments for shaker tests on lightweight structures were illustrated. In detail the following phenomena could be highlighted:

- Mass loading of test item through seismic part of the load cell (i.e. the mass portion of the load cell between the test item and the force measurement plane of the load cell)
- Friction in interface region between test item and force cell due to micro-slip
- Coupling of transverse and rotational stinger stiffnesses into test item

According to these phenomena, the following best practices for shaker attachments can be derived:

- Minimization of load cell mass
- Incorporation of seismic part of load cell into FE model *or* structural modification of identified experimental modal model to compensate the effects of the load cell mass (as a rule of thumb, half of the nominal overall mass of the load cell usually appears to be a reasonable estimate for the seismic part, if no detailed information is available)
- Bolting or gluing of load cell to test item such that minimal friction can occur in the interface region
- Decoupling of transverse and rotational stinger stiffnesses from test item (the axial stiffness will always be decoupled through the axial force measurement of the load cell)

Especially the last point can confront the test engineer with the greatest challenges. In the example above, the vinyl stinger obviously was a good choice. However, this stinger type is very flexible also in axial direction and may not be suited for all frequency ranges and/or test item masses. In detail, considering the stinger as an axial spring and the test item as a lumped mass, excitation of this one-mass-oscillator beyond its natural frequency will become increasingly difficult because of the decoupling effect (mechanical filter). Also, vinyl material tends to dissipate energy more than other stinger materials which in addition limits its applicability.

To that extend the steel stinger is more appropriate. But one must be aware, that transverse and rotational coupling is much stronger as well. In case of close by structural modes and stinger modes this can lead to a significant disturbance of the modal behavior of the test item. Thus, a solution with high axial stiffness, moderate energy dissipation, and sufficient decoupling is usually sought. The best solution here is to design stingers with a stiff tube that takes up most of the length of the stinger in combination with flexible, joint like end sections. A typical stinger of this type is shown in Figure 18. With sufficient knowledge of the used materials, these stingers can perfectly be designed for a specific test e.g. with the help of FE analyses.

Figure 18: Example of designed stinger – stiff tube (CFRP) and joint like end sections (steel)

Taking into account the proposed suggestions should effectively limit the adverse effects of stinger attachments on shaker tests of lightweight structures.